 CMES, vol.64, no.2, pp.213-226, 2010

Size-Dependent Behavior of Macromolecular Solids I: Molecular Origin of the Size Effect

W. Wei[1] **and David C.C. Lam**[1]

Abstract: Molecular rotation is the elastic deformation mechanism underpinning macroscopic deformation in macromolecular solid. In this investigation, molecular mechanic simulations are used to investigate the effect of size on the higher order material properties macromolecular solid. The rotational behavior of molecular coils embedded in beams was examined as a function of the beam size in tension, and in bending where the strain gradients in the bent direction are size-dependent. Analysis showed that the effective elastic modulus is size dependent when strain gradients are significant in bending, but not in tension. Analysis of the molecular rotation behavior indicated that the increase in the effective elastic modulus is generated by increase in molecular rotations with strain gradients. This implies that the higher order strain gradient stiffening has the same underlying deformation mechanism as conventional elastic deformation. Further analysis confirmed that the individual higher order material length scale parameter l_2 is uniquely related to the elastic modulus of individual solid studied. These results suggested that size-stiffening in polymers is not a new deformation mechanism, but is a new association of strain gradients with molecular rotations in the solid.

1 Size stiffening mechanics

Conventional view of mechanical deformation is based on displacement at a point [Fung and Tong (2001)]. This mathematical approach is valid for solids where the rotational characteristics at the point is negligible [Ashby (1970)]. When the solid cannot be modeled as collections of points, but must be considered as atoms with directionality, higher order mechanics that account for rotations at the atom are needed.

Strain gradient mechanics has been used successfully to model the size dependence of elastic stiffness in nanofibers, nanoporous solids and nanocomposites [Arinstein

[1] Department of Mechanical Engineering, The Hong Kong University of Science and Technology, Clear Water Bay, Kowloon, Hong Kong SAR China. Email:david.lam@ust.hk

et al (2007); Ji et al (2006); Yang et al (2006); Lu et al (1994)]. The success was developed on the basis of the modified strain gradient elasticity theory [Lam et al (2003)]. In classical strain gradient theories [Mindlin (1968)], 18 strain gradient terms were grouped without consideration for the character of dilatation, stretch and rotation in the gradients [Fleck et al (1994)]. The work density in this case is written as,

$$w = \frac{1}{2}k\varepsilon_{ii}\varepsilon_{jj} + \mu\varepsilon'_{ij}\varepsilon'_{ij} + a_1\eta_{ijj}\eta_{ikk} + a_2\eta_{iik}\eta_{kjj} + a_3\eta_{iik}\eta_{jjk} + a_4\eta_{ijk}\eta_{ijk} + a_5\eta_{ijk}\eta_{kji} \quad (1)$$

where

$$\varepsilon_{ij} = \frac{1}{2}\left(\partial_i u_j + \partial_j u_i\right), \quad (2)$$

and u_i is the displacements, k and μ are the bulk and shear moduli, respectively, and a_i are material length scale parameters, the deviatoric strain, ε'_{ij} is,

$$\varepsilon'_{ij} = \varepsilon_{ij} - \frac{1}{3}\varepsilon_{mm}\delta_{ij}, \quad (3)$$

and the strain gradient is,

$$\eta_{ijk} = \partial_{ij}u_k. \quad (4)$$

a_i, the material length scale parameters were mixed in character. Lam et al (2003) modified the theory by regrouping the strain gradients according to their character into pure dilatation, stretch and rotation gradients. The work density in the modified theory is,

$$w = \frac{1}{2}k\varepsilon_{ii}\varepsilon_{jj} + \mu\varepsilon'_{ij}\varepsilon'_{ij} + \mu l_0^2\varepsilon_{mm,i}\varepsilon_{nn,i} + \mu l_1^2\eta^{(1)}_{ijk}\eta^{(1)}_{ijk} + \mu l_2^2\chi^s_{ij}\chi^s_{ij}, \quad (5)$$

and the dilatation, stretch and rotation gradients are associated with l_0, l_1 and l_2, respectively.

In polymers, macromolecular chains in the solid deform via molecular rotations. When the chains are strained, the macromolecules uncoil by rotating the molecular segments into new configurations [Treloar (2005)]. The configurational change is modeled using statistical mechanics such that the shear modulus of a network of polymer is given as

$$\mu = \frac{\rho RT}{M_c}, \quad (6)$$

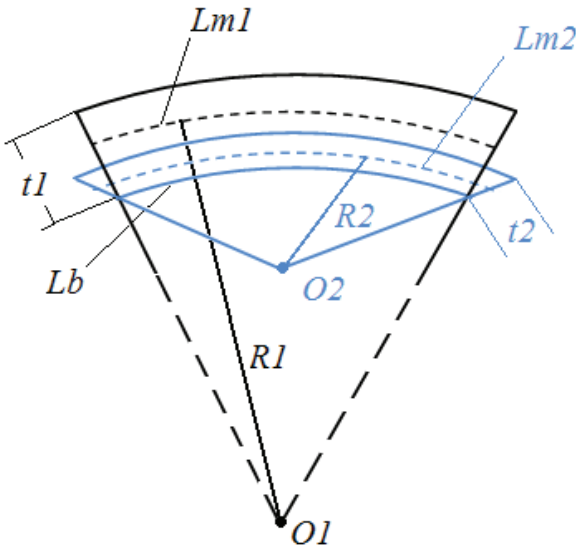

Figure 1: Gradients of strain in thin beam is larger than thick beam. L_{m1} and L_{m2} are the neutral axes of the thick and thin beam, respectively

where ρ is the density, M_c is the segmental molecular weight, R is the Avogadro constant and T is the temperature in K. In this model, molecular rotations occur in response to strains between the nodes, but the nodes are regarded as point nodes such that the rotations at the nodes are ignored. the rotations at the node are not free, but are constrained by connected chains. The rotations between atomic nodes are characterized in higher order mechanics by the symmetric rotation gradient. The deformation energy is given as,

$$w = \frac{1}{2}k\varepsilon_{ii}\varepsilon_{jj} + \mu\varepsilon'_{ij}\varepsilon'_{ij} + \mu l_2^2 \chi^s_{ij}\chi^s_{ij}, \tag{7}$$

where l_2 is the material length scale parameter for rotation gradients in the polymer [Yang et al (2002)]. Stiffening occurs when is non-negligible.

Rotation gradients are significant when the beam is thin. The effective elastic modulus E_{eff} with rotational stiffening is [Lam et al (2003)],

$$E_{eff} = E_o\left[1 + 3(1-\nu)\frac{l_2^2}{h^2}\right], \tag{8}$$

where E_o is the conventional elastic modulus, h, is the thickness of the beam and l_2 is the higher order length scale parameter associated with rotational gradients [Sun

et al (2008)]. The equation has been shown to be in good agreement with bending experiment data [Cuenot et al (2000); Gu et al (2005); Wang and Lam (2010]. In addition, the higher order theory had also been used to explain the size dependence observed in nanocomposites [Wang and Lam (2010)] and *n* anostiffening behavior in nanoporous solids [Wang and Lam (2009)].

In this investigation, we examined the deformation energy density as a function of the rotational changes in different molecular solids, including polyethylene (PE), styrene butyl rubber (SBR) and nylon 6 (Nylon) using molecular mechanics. The dependence of l_2 on the molecular character of the chains is studied as a function of rotation gradient to examine the molecular origin of size-stiffening in macromolecular solids.

2 Modeling approach

Deformation in metals [Cleri and Rosato (1993)], semiconductors [Giannozzi et al (1991)] and ceramics, and small molecules, can be modeled using *ab initio* methods where Hamiltonian functions are solved and optimized. The approach is suitable for the simulations of small collections of atoms, molecules and short macromolecular segments, but is unsuited for large molecules because of computational demands. Macromolecular solids can be modeled using molecular models [Maranganti and Sharma (2007)]. To study the deformation energy behavior from the molecular perspective, molecular rotation as a function of deformation can be efficiently simulated using molecular mechanics. The molecular rotations before and after deformation are simulated in this study using the Forcite Plus module in Material Studio [Material's studio 4.4]. In the undeformed state, macromolecules are generally coiled. Pulling the ends apart will neither lengthen nor change the bond angles of the covalent bonds, but will rotate and uncoil the chain into higher energetic configurations. An idealized case of entangled or crosslinked coils is shown on the left in Figure 2 and an isolated coil is shown on the right.

To study the deformation behavior of the macromolecules with and without strain gradients, the macromolecular coils were embedded into beams (Figure 3), and their changes in deformation energy density as a function of beam thickness were examined in bending and in tension. Tension is simulated by imposing the requisite displacements to the anchor points of the coil segments (Figure 3). When bent, the coils further away from the neutral axis are stretched. The rotations of the carbon atoms between the anchor atoms are unconstrained and can rotate freely to adapt a minimum energy configuration. The anchors, which are crosslinked or entangled, are constrained from free rotation by the connected neighboring chains. Its position is prescribed in the simulation according to conventional bending mechanics [Fung

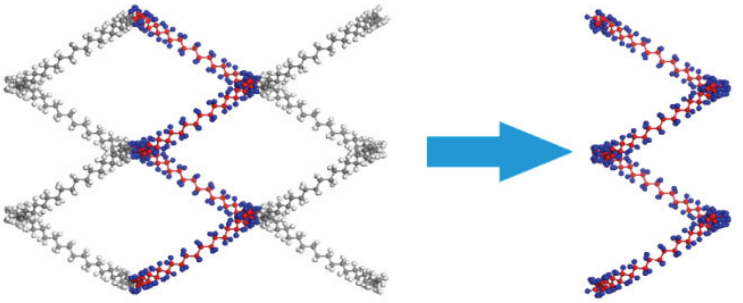

Figure 2: Front view of an idealized network of macromolecular chains (left) and a single coil (right).

(1977)] via,

$$\begin{aligned} \varepsilon_z &= \kappa x \\ \varepsilon_x = \varepsilon_y &= -\nu\varepsilon_z = -\nu\kappa x \\ \gamma_{xy} = \gamma_{yz} &= \gamma_{zx} = 0 \end{aligned} \tag{9}$$

where

$$\kappa = \frac{1}{R} = \frac{L_m - L_b}{L_m}\frac{2}{h}. \tag{10}$$

The relations between the strain and the positions of the anchors at different location r before and after deformation [Timoshenko and Goodier (1987)] is,

$$\varepsilon_x = \frac{|x'_r - x_r|}{|x_r|} \quad \varepsilon_y = \frac{|y'_r - y_r|}{|y_r|} \quad \varepsilon_z = \frac{|z'_r - z_r|}{|z_r|}. \tag{11}$$

The undeformed positions are unprimed while the deformed positions are primed (Figure 3). In bending, a gradient of strain is developed along the thickness; and the rotation at the anchors in one layer would be affected by segmental rotations in the adjacent layer.

3 Benchmarking

Using this model, the additional rotational energies that were not accounted for in conventional strain-based mechanics are tracked as a function of the deformation

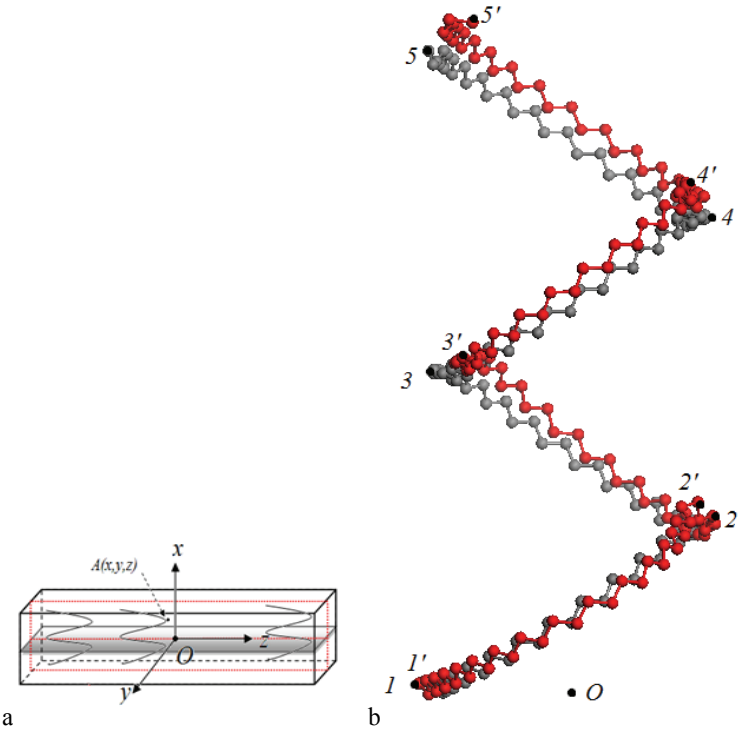

Figure 3: a) Macromolecular coils in beam and b) the coil before (unprimed nodes) and after bending (primed nodes) in bottom schematic.

and thickness in our model. The deformation energy density per volume, u, is calculated via,

$$u = \frac{\Delta U \rho}{m}, \tag{12}$$

where m is the mass of the coil segment, ρ is the density of the polymer, and ΔU is the difference in energy before and after deformation. In classical mechanics, u is a function of the bent curvature [Norton (2006)],

$$u = \frac{1+2\nu^2}{2} E \varepsilon_z^2 = \frac{1+2\nu^2}{2} E \kappa^2 x^2, \tag{13}$$

where x is the location of the coil along the thickness direction such that E can be determined from a plot of u versus κ. The validity of the simulation is checked by

comparing the E with experimental data. Since data from experiments are given as size-independent shear modulus μ_o. The elastic modulus is converted into shear modulus for comparison in Table 1. The settings used in the simulation are also shown. Comparison of the shear moduli showed that the simulation results are within 10% agreement with reported values for all three polymers modeled.

Table 1: The parameters used in our simulation model setting. The experimental data is from Boháč and Vretenár ; Bartczak, Argon, Cohen and Weinberg (1999)

	PE	SBR	Nylon
Stoichiometry	CH_2	$C_{32}H_{44}$	$C_{12}H_{24}N_2O_2$
m_0 *(g/mol)*	14	428	228
Poisson's ratio	0.5	0.5	0.5
r *(g/cm*^{3}*)*	0.9565	1.046	1.15
*R (N*m/K*mol)*	8.314	8.314	8.314
$T(K)$	297	297	297
Experimental μ_0 (GPa)	2.52E-1	7.67E-3	3.7E-3
Simulation μ_0 (GPa)	2.32E-1	7.71E-3	3.19E-3

4 Results and Analysis

4.1 Mechanistic basis for higher order deformation

Strain gradients become significant when the beam thickness is reduced. The effect of the thickness on the energy density in PE beam in bending is shown in Figure 4. The plot showed that the rate of energy change increases with thickness when the thickness is less than 150 μm, but becomes independent of thickness at larger thickness. Using equation (13), the effective elastic modulus can be determined from Figure 4. The effective moduli normalized by the thickness-independent elastic modulus, E_o, are plotted in Figure 5 as a function of thickness. Figure 5 showed that without strain gradients, the effective moduli are independent of thickness, but with strain gradients, the effective moduli become thickness dependent. Thus, the increase in energy with beam thickness in Figure 4, and the increase in the effective elastic moduli in Figure 5 is due to non-negligible strain gradients generated in the beam during bending.

Molecularly, the changes in energy come from molecular rotations. The normalized cumulative difference in rotation as a function of beam thickness is shown in Figure 6. The figure showed that the molecular rotation increased with decrease in

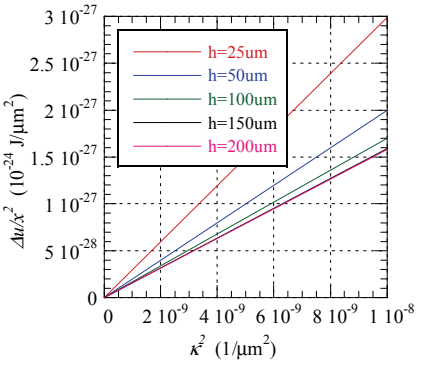

Figure 4: Effect of thickness on energy density in PE beams in bending.

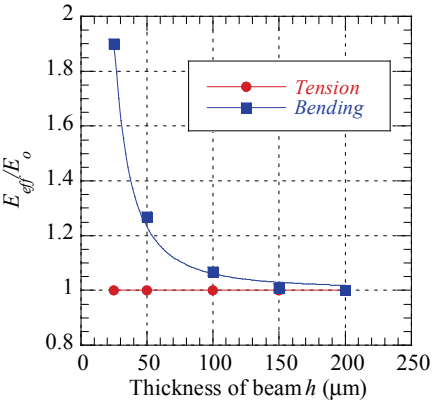

Figure 5: Effective elastic modulus of PE as a function of beam thickness under tension and bending. E_o is the elastic modulus in tension.

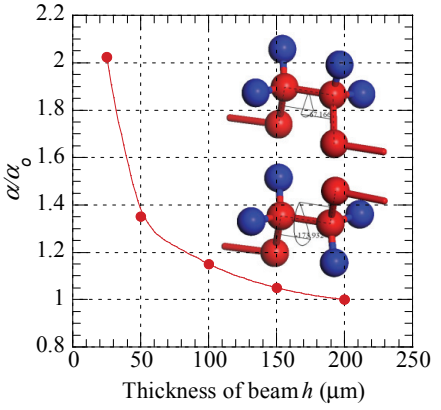

Figure 6: The molecular rotation before (up) and after (down) deformation and its size dependence on beam thickness. α_0 is the cumulative rotation for thick beam.

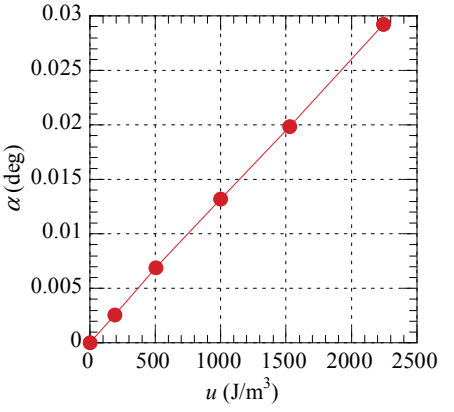

Figure 7: Relationship between average molecular rotation and deformation energy density taken from beams with different thicknesses. The slope is λ.

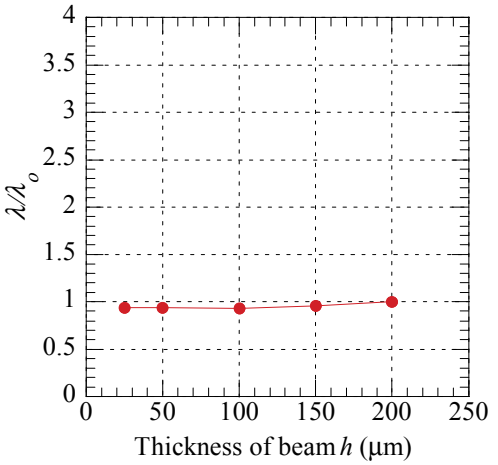

Figure 8: Effect of beam thickness on λ where λ_0 is the value at $h = 200\mu$m.

thickness. A cross plot of the deformation energy density and molecular rotation is shown in Figure 7. The plot showed that rotations are linearly related to deformation energy density. More importantly, the rate of change between the two, λ (=u/α), is constant (Figure 8). This means that the increase in deformation energy density with thickness is associated with molecular rotation and that molecular rotation is the underlying molecular mechanism behind strain gradient deformation.

4.2 Relation between μ and l_2

Since both strain gradient and strain deformation generate molecular rotations and rotation energy in a molecular segment. It would be instructive to examine if l_2 shares the same molecular dependence as μ_o. The elastic modulus, and by corollary, the shear modulus of a macromolecular solid is known to decrease with increase in the molecular weight of the chain (equation (6)). The amount of rotation per carbon atom would be reduced resulting in lower rotation energy when the molecular weight of the chain is increased. Using the developed model, the effect of molecular weight is examined in three macromolecules, polyethylene, styrene butyl rubber and nylon 6. The molecular weight of PE is increased from 8 to 122 units of the monomer, from 5 to 78 units for SBR and 7 to 45 units for nylon 6. μ_o is shown to increase linearly with $1/n$ (Figure 9 to Figure 11). Cross-plotting μ_o and l_2 showed that the two are linearly related (Figure 12 and Figure 13). These plots showed their ratios $\beta = l_2 \mathrm{v} \mu$ changes with chemistry, but is independent of the molecular weight. This means that once β is known for a molecular solid with a

specific chemistry, l_2 for the solid different molecular weight can be projected from the constant and μ_o.

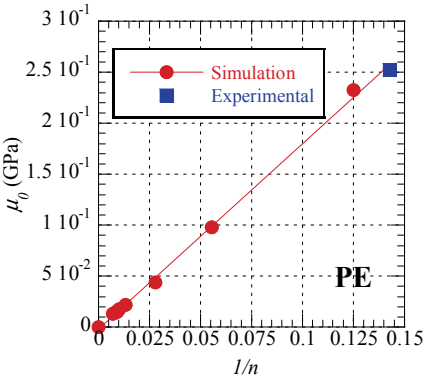

Figure 9: Shear modulus as a function of $1/n$ in the PE system. The solid square is the experimental data for PE shown in Table 1.

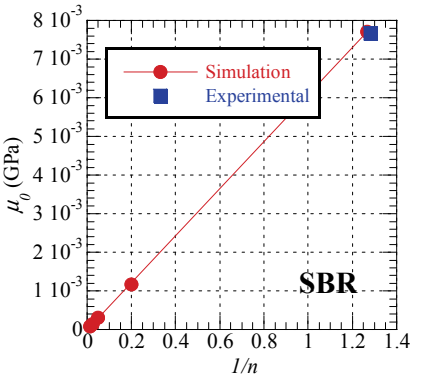

Figure 10: Shear modulus as a function of $1/n$ in the SBR system. The solid square is the experimental data for SBR shown in Table 1.

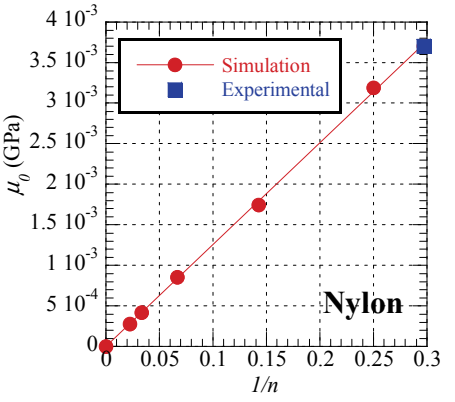

Figure 11: Shear modulus as a function of $1/n$ in the Nylon system. The solid square is the experimental data for Nylon shown in Table 1.

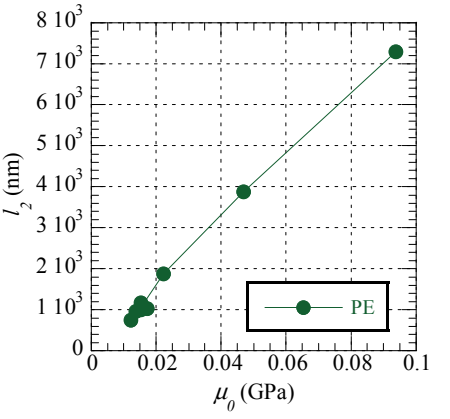

Figure 12: l_2 as a function of μ_0 in the PE system.

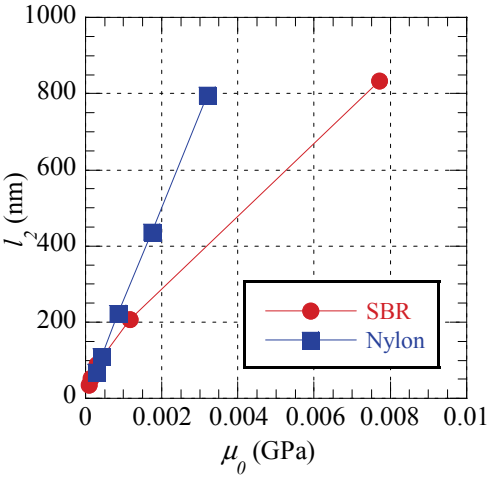

Figure 13: l_2 as a function of μ_0 in the SBR & Nylon system.

5 Remarks

In this investigation, we examined the rotational behavior of molecules using molecular mechanic model and showed that the rotation energy per unit rotation is the same regardless of whether the rotation is generated with strain alone, or with strains and rotation gradients. The results were obtained using an idealized coil model. The fixed coil approach allowed effective examination of the rotations before and after deformation, but cannot simulate dynamic chain interactions well. The behaviors of interactions between chains in entangled thermoplastic and cross-linked thermosets are examined using dynamic simulations and are reported in companion papers in this series.

6 Conclusions

Molecular mechanics was used to simulate conventional and higher order size-dependent elastic deformation behavior. The elastic moduli in bending and in tension in thick beams were shown to be identical. When the beam thickness is reduced, the elastic modulus of the beam in tension remains the same while the beam in bending showed an effective increase that is inversely proportional to the beam thickness. The higher order material length scale parameters, l_2, delineated from the size-dependence were shown to be associated with molecular rotation. The rotation energy per unit rotation in the molecular segments in thin beams was shown to be the same in thick beam where only strains are active. The results

confirmed that strain-based deformation and higher order deformation shared the same molecular rotation deformation mechanism. Investigation on the character of the higher order behavior showed that l_2 is uniquely related to the elastic shear modulus; and this behavior is shown to be consistent in polyethylene, polyimide and styrene butyl rubber. These results indicate that the higher order elastic deformation behavior in macromolecular solids is not a new mechanism, but is a new association between the molecular rotation mechanism and the rotation gradients in the solid.

Acknowledgement: This work was supported by the Research Grants Council of the Hong Kong Special Administrative Region, the People's Republic of China under projects HKUST 615007 and 615505.

Reference

Arinstein, A.; Burman,M.; Gendelman, O.; Zussman, E. (2007). Effect of supramolecular structure on polymer nanofibre elasticity. *Nature Nanotechnology* vol. 2, no. 1, pp. 59-62.

Ashby, M. F. (1970). The Deformation of Plastically Non-homogeneous Materials. *Philosophical Magazine* vol. 21, pp. 399-424.

Bartczak, Z.; Argon, A. S.; Cohen, R. E.; Weinberg, M. (1999). Toughness mechanism in semi-crystalline polymer blends: II. High-density polyethylene toughened with calcium carbonate filler particles. *Polymer* vol. 40, no. 9, pp. 2347-2365.

Bohá, V.; Vretenár, V. Thermophysical properties of styrene butadiene rubber filled with pine tree particles measured by the transient plane source technique. from `http://www.tpl.fpv.ukf.sk/engl{\_}vers/thermophys/2004/Boh-Vre.pdf`.

Cleri, F.; Rosato, V. (1993). Tight-Binding Potentials for Transition-Metals and Alloys. *Physical Review B* vol. 48, no. 1, pp. 22-33.

Cuenot, S.; Demoustier-Champagne, S.; Nysten, B. (2000). Elastic modulus of polypyrrole nanotubes. *Physical Review Letters* vol. 85, no. 8, pp. 1690-1693.

Fleck, N. A.; Muller, G. M.; Ashby, M. F.; Hutchinson, J. (1994). Strain Gradient Plasticity - Theory and Experiment. *Acta Metallurgica Et Materialia* vol. 42, no. 2, pp. 475-487.

Fung, Y. C. (1977). A first course in continuum mechanics. Englewood Cliffs, N.J., Prentice-Hall.

Fung, Y. C.; Tong, P. (2001). Classical and computational solid mechanics. Singapore; Hong Kong, World Scientific.

Giannozzi, P.; Degironcoli, S.; Pavone, P.; Baroni, S. (1991). Abinitio Calculation of Phonon Dispersions in Semiconductors. *Physical Review B* vol. 43, no. 9, pp. 7231-7242.

Gu, S. Y.; Wu, Q. L.; Ren, J.; Vancso, G. J. (2005). Mechanical properties of a single electrospun fiber and its structures. *Macromolecular Rapid Communications* vol. 26, no. 9, pp. 716-720.

Ji, Y.; Li, B. Q.; Ge, S. R.; Sokolov, J. C.; Rafailovich, M.H. (2006). Structure and nanomechanical characterization of electrospun PS/clay nanocomposite fibers. *Langmuir* vol. 22, no. 3, pp. 1321-1328.

Lam, D. C. C., Yang, F.; Chong, A. C. M.; Wang, J.; Tong, P. (2003). Experiments and theory in strain gradient elasticity. *Journal of the Mechanics and Physics of Solids* vol. 51, no. 8, pp. 1477-1508.

Lu, T. J.; Z. C. Xia; J. W. Hutchinson (1994). Delamination of Beams under Transverse-Shear and Bending. *Materials Science and Engineering a-Structural Materials Properties Microstructure and Processing* vol. 188, no. 1-2, pp. 103-112.

Maranganti, R.; Sharma, P. (2007). A novel atomistic approach to determine strain-gradient elasticity constants: Tabulation and comparison for various metals, semiconductors, silica, polymers and the (Ir) relevance for nanotechnologies. *Journal of the Mechanics and Physics of Solids* vol. 55, no. 9, pp. 1823-1852.

Material's Studio 4.4. Forcite. from `http://accelrys.com/products/datasheets/forcite.pdf`.

Mindlin, N. (1968). On first strain gradient theories in linear elasticity. *International Journal of Solids and Structures* vol. 4, pp.109-124.

Norton, R. L. (2006). Machine design :an integrated approach. Upper Saddle River, NJ, Prentice Hall.

Sun, L.; Han, R. P. S.; Wang, J.; Lim, C. T. (2008). Modeling the size-dependent elastic properties of polymeric nanofibers. *Nanotechnology* vol. 19, no. 45, pp. 1-8.

Timoshenko, S.; Goodier, G. N. (1987). Theory of elasticity. New York, McGraw-Hill.

Treloar, L. R. G. (2005). The physics of rubber elasticity. Oxford, Clarendon Press.

Wang, J.; Lam, D .C. C. (2009). Model and analysis of size-stiffening in nanoporous cellular solids. *Journal of Materials Science* vol. 44, no. 4, pp. 985-991.

Wang, J.; Lam, D .C. C. (2010). Nanostiffening in Polymeric Nanocomposites. *CMC* vol. 471, no. 1, pp.1-18

Yang, F.; Chong, A. C. M.; Lam, D. C. C.; Tong, P. (2002). Couple stress based strain gradient theory for elasticity. *International Journal of Solids and Structures* vol. 39, no. 10, pp. 2731-2743.

Yang, F. Q. (2006). Effect of interfacial stresses on the elastic behavior of nanocomposite materials. *Journal of Applied Physics* vol. 99, no. 5, 054306-1–054306-5.